

Increased expression of S100A6 is associated with decreased metastasis and inhibition of cell migration and anchorage independent growth in human osteosarcoma

Hue H. Luu^a, Lan Zhou^{a,b}, Rex C. Haydon^a, Andrea T. Deyrup^c, Anthony G. Montag^{a,d},
Dezheng Huo^e, Robert Heck^f, Claus W. Heizmann^g, Terrance D. Peabody^a,
Michael A. Simon^a, Tong-Chuan He^{a,*}

^aMolecular Oncology Laboratory, Department of Surgery, The University of Chicago Medical Center, Chicago, IL, USA

^bDepartment of Biomedical Engineering, Chongqing University of Medical Sciences, Chongqing, China

^cDepartment of Pathology and Laboratory Medicine, Emory University, Atlanta, GA, USA

^dDepartment of Pathology, The University of Chicago Medical Center, Chicago, IL, USA

^eDepartment of Health Studies, The University of Chicago, Chicago, IL, USA

^fDepartment of Orthopaedic Surgery, Campbell Clinic, Germantown, TN, USA

^gDivision of Clinical Chemistry and Biochemistry, Department of Pediatrics, University of Zurich, Zurich, Switzerland

Received 10 November 2004; received in revised form 27 January 2005; accepted 12 February 2005

Abstract

While most osteosarcoma patients have metastatic or micrometastatic lesions, less than 15% of them have clinically detectable metastatic diseases at presentation. To identify potential markers that may predict osteosarcoma metastasis, we analyzed the expression of S100A6 in 50 osteosarcoma cases and found that 84% of the analyzed specimens stained positive for S100A6. There is a trend towards decreased clinically evident metastasis with increased S100A6 staining. Overexpression of S100A6 in osteosarcoma cells decreases cell motility and anchorage independent growth on collagen gels. Our findings provide evidence that, while S100A6 is commonly overexpressed in human osteosarcoma, loss of its expression correlates with a metastatic phenotype.

© 2005 Elsevier Ireland Ltd. All rights reserved.

Keywords: Osteosarcoma; S100A6; EF-hand proteins; Metastasis; Cell motility; Anchorage independent growth

1. Introduction

Osteosarcoma is the most common primary malignancy of bone, with a peak incidence in the second decade of life [1,2]. With the current treatment for osteosarcoma, which includes wide resection and chemotherapy, the average 5-year disease-free survival rate is 55–60% [3,4]. At the time of diagnosis,

* Corresponding author. Address: Molecular Oncology Laboratory, Department of Surgery, The University of Chicago Medical Center, 5841 South Maryland Avenue, MC3079, Chicago, IL 60637, USA. Tel.: +1 773 702 7169; fax: +1 773 834 4598.

E-mail address: tche@surgery.bsdu.uchicago.edu (T.-C. He).

80% of osteosarcoma patients have micrometastatic or clinically detectable metastatic disease [5,6]. However, current radiographic imaging modalities are only able to detect approximately 8–15% of the patients [7,8]. One of the challenges in the management of patients with osteosarcoma is to identify the 20% of patients who do not have micrometastatic disease at diagnosis. The ability to identify these patients at initial presentation could alter the treatment protocols such as chemotherapy [9].

The genetic events that lead to the development of osteosarcoma are not known [10–12]. Understanding of this process may identify potential markers for osteosarcoma. To this end, amplifications and/or rearrangements of the region 1q21–1q22 have been observed in human bone and soft tissue sarcomas [10,11,13–15]. A cluster of at least 16 types of S100 genes is located on 1q21. The S100 protein family constitutes a group of nearly 20 proteins that contain well-conserved EF-hand calcium binding domains [16–20]. The first member of this protein family was isolated from bovine brain tissue and was called bovine brain S100 protein because of its solubility in a 100% saturated solution of ammonium sulfate [21]. The S100 proteins, with molecular weights between 9 and 14 kDa, have been shown to interact with transcriptional factors and may be involved in the regulation of protein phosphorylation, calcium homeostasis, cell proliferation, and differentiation [16,18,19]. S100 proteins have also been shown to interact with the cytoskeleton and may thereby influence cell motility [18,19,22–26].

Several S100 proteins have been associated with human cancers. Expression of S100A2 is decreased in human breast and laryngeal carcinomas and melanoma, but increased in gastric cancer [27–30]. S100A4 is highly expressed in advanced colon, breast, esophageal, and nonsmall cell lung cancers, while S100A7 is highly expressed in gastric cancer [30–34]. Furthermore, several S100 proteins are used clinically as immunohistochemical markers to identify and classify multiple tumors, including neuroendocrine tumors, thyroid carcinoma, melanoma, renal carcinoma, teratomas, Langerhans histiocytosis, pheochromocytoma, and cartilage forming tumors [35–37]. In addition, S100A4 has been shown to upregulate matrix metalloproteinase-2 in osteosarcoma to confer a more metastatic phenotype [38].

As a part of an ongoing effort to understand the roles of several members of the S100 protein family in human osteosarcoma, we here report our findings on S100A6. Like other members of its family, S100A6 (a.k.a., calylin) is over-expressed in several human tumors, including human melanoma, squamous cell carcinoma, malignant fibrous histiocytoma (MFH), and carcinomas of the thyroid, breast, and colon [36,39]. Taking into account the reports of amplifications of 1q21–22 in human osteosarcoma, the localization of S100 gene cluster in that region, and the association of S100 proteins with a number of human cancers, we hypothesized that S100A6 would be involved in the pathogenesis of osteosarcoma. Our findings indicate that S100A6 is expressed in the vast majority of human osteosarcoma, and that increased S100A6 expression correlates with a lower occurrence of metastatic disease. Overexpression of S100A6 inhibits the cell migration and anchorage-independent growth of human osteosarcoma cells, suggesting that S100A6 may play a role in regulating osteosarcoma metastasis.

2. Materials and methods

2.1. Tissue culture and chemicals

HEK293 and human osteosarcoma lines 143B, MNNG/HOS, and TE85 were purchased from ATCC (Manassas, VA). HEK293 cells were maintained in complete Dulbecco's Modified Eagle's Medium (DMEM) containing 10% FCS (fetal calf serum, HyClone, Logan, UT). MNNG/HOS, TE85 and 143B lines were maintained in complete Minimum Essential Medium Eagle (EMEM) supplemented with 10% FCS, 2.0 mM L-glutamine (Mediatech), 1 × nonessential amino acids (Mediatech), 1.0 mM sodium pyruvate (Mediatech) at 37 °C in 5% CO₂. Unless otherwise indicated, all chemicals were purchased from Sigma (St Louis, MO) or Fisher Scientific (Pittsburgh, PA).

2.2. Osteosarcoma samples and patients

The use of human tumor specimens followed the guidelines approved by the Institutional Review

Board of the University of Chicago. Fifty osteosarcoma samples corresponding to 50 patients from pre-chemotherapy biopsies or post-chemotherapy primary resections/amputations were randomly selected and diagnosis verified by a pathologist for our analysis. Subsequent samples from the same patient (i.e. recurrent lesions or duplicated samples) or specimens that were not biopsies or primary resections were not included. All biopsy specimens were never exposed to chemotherapy while all primary resection samples had been exposed to chemotherapy. Each of the samples examined in our investigation is from a different patient. The 50 samples represented a cross-section of the different osteosarcoma histologic subtypes and were obtained between 1987 and 1999. The standard treatment regimen for these patients included biopsy, followed by neo-adjuvant chemotherapy, primary wide or radical resection/amputations, and then an additional course of chemotherapy. The chemotherapeutic agents used evolved over the 12 years the samples were collected and included combinations of methotrexate, doxorubicin, ifosfamide/MESNA, carboplatin, and/or cisplatin. Clinical data including survival and the presence of metastatic disease at diagnosis and follow-up were available for statistical analysis. In 26 of the 50 patients, the post-chemotherapy tumor viability (range 0–95%) was also available for review. In the remaining 24 patients, data on post-chemotherapy tumor viability was unavailable. There were inconsistent reports of the tumor margins and could not be included in the analysis. The median follow-up time was 84 months (range 30–168 months).

2.3. Immunohistochemical staining with S100A6 antibody

Immunohistochemical staining was performed as previously described [40]. Briefly, paraffin-embedded sections were deparaffinized using xylene at room temperature and then gradually rehydrated. Antigen retrieval on the deparaffinized sections was performed by immersing the samples in 0.1 M citrate buffer (pH 6.0), boiling the samples in the microwave for 10 min, and then allowing the samples to cool to room temperature. The samples were fixed in acetone. Endogenous peroxidase activity was blocked by immersing the samples in methanol containing 3%

hydrogen peroxide for 12 min. Next, the samples were blocked in FCS for 20 min. The goat anti-human recombinant S100A6 antibody, previously characterized by Ilg et al., was used at a 1:200 dilution in 4% powdered skim milk [36], incubated for 1 h at room temperature, washed in phosphate buffered saline (PBS) three times for 2 min each, and then blocked again with FCS for 15 min. The slides were incubated in biotinylated anti-goat secondary antibody (Super Sensitive Link, BioGenex, San Ramone, CA) at room temperature for 20 min and then washed in PBS four times for 5 min each. Streptavidin conjugated peroxidase (Super Sensitive Label, BioGenex) was added for 20 min. The samples were then washed in PBS for 20 min as described. To visualize the S100A6 protein, a diamino-benzidine substrate (Vector Laboratories, Burlingame, CA) was added for 20 min followed by counterstaining with light green and mounting in Permount (Fisher Scientific). Negative controls were performed with goat IgG antibody (PIERCE, Rockford, IL) and no primary antibody. Two investigators (HHL and AGM) independently scored the slides for the staining intensity and agreed on the staining scores for all of the slides, as previously described [40,41]. Scoring of the slides was performed prior to the collection of any patient information and therefore was blinded to the clinical data. The staining score was rated as 0 (no staining), 1+ (weak), 2+ (moderate), or 3+ (strong) based on the intensity of the staining pattern. Staining score 0 was defined as no staining visible. Staining score 1+ was defined as light staining requiring high power (200×) to identify the staining pattern. Staining score 2+ was defined as moderate staining requiring medium power (100×) to identify the staining pattern. Staining score 3+ was defined as dark staining visible on low power (40×).

2.4. Construction of S100B, S100A2, S100A4, and S100A6 expression vectors

The cDNA coding regions corresponding to human S100B, S100A2, S100A4, and S100A6 were PCR amplified from human cDNA libraries with the following oligonucleotides: for S100B, 5'-CTA GCT AGC GAT GTC TGA GCT GGA GAA GGC-3' and 5'-CGC GGA TCC TCA CTC ATG TTC AAA GAA C-3'; for S100A2, 5'-CTA GCT AGC CAT GAT GTG CAG TTC TCT GGA GC-3' and 5'-CGC GGA

TCC TCA GGG TCG GTC TGG GCA GCC-3'; for S100A4, 5'-CTA GCT AGC CAT GGC GTG CCC TCT GGA GAA G-3' and 5'-CGC GGA TCC TCA TTT CTT CCT GGG CTG CTT ATC-3'; for S100A6, 5'-CTA GCT AGC CAT GGC ATG CCC CCT GGA TC-3' and 5'-CGC GGA TCC TCA GCC CTT GAG GGC TTC ATT G-3'. Amplified fragments were subcloned into a CMV-driven expression vector with an N-terminal double HA tag, resulting in pHAHA-S100B, pHAHA-S100A2, pHAHA-S100A4, and pHAHA-S100A6. All PCR amplified fragments were verified by DNA sequencing. Cloning and construction details of the above vectors are available upon request.

2.5. Construction of a recombinant adenoviral vector expressing S100A6

The cDNA encoding human S100A6 was subcloned into the pAdTrack-CMV vector, resulting in pAdTrack-S100A6. Recombinant adenovirus expressing S100A6 (i.e. AdS100A6) was generated as previously described [42]. It is noteworthy that the AdS100A6 virus also expressed GFP allowing easy detection of gene transduction efficiency upon infection.

2.6. Cell transfections and Western blotting analysis

The experimental procedure was conducted as described [43]. Subconfluent HEK293 cells were transfected with S100 expression vectors using LipofectAMINE (Invitrogen, Carlsbad, CA). At 24 h after transfection, the cells were collected and lysed in Laemmli sample buffer. Cleared total cell lysate was denatured by boiling and loaded onto a 4–20% gradient or 8% SDS-polyacrylamide gel (approx. 10 µg total proteins per lane). After electrophoretic separation, proteins were transferred to an Immobilon-P membrane (Millipore, Bedford, MA) via electroblotting. The membrane was blocked with 5% nonfat milk in TBST (10 mM Tris-HCl, pH 8.0, 150 mM NaCl, 0.05% Tween-20) at room temperature for 1 h and probed with an anti-HA antibody (Roche Molecular Biochemicals, Indianapolis, IN) or the anti-S100A6 antibody for 60 min, followed by a 30-min incubation with an anti-mouse or anti-goat IgG secondary antibody conjugated with

horseradish peroxidase (PIERCE). The presence of S100A6 protein or HA-S100 proteins was detected by using the SuperSignal West Pico Chemiluminescent Substrate kit (Pierce) and recorded using the Kodak 440CF ImageStation.

2.7. Cell wounding assay

The experiments were carried out essentially as described previously [44]. Subconfluent TE85, MNNG/HOS, and 143B cells were plated into 12-well tissue culture plates and allowed to attach with complete media with 10% FCS for 3 h. Cells were washed with serum free media and cultured with 0.0, 0.1, 0.5, or 1% FCS, and infected with either AdS100A6 or AdGFP at a comparable titer. At 20 h after infection, the monolayer of cells was wounded using micropipet tips. Marks were created on the plates using 18-gauge needles as reference points for serial imaging. Bright field and fluorescence images of the exact field were taken at 0, 5, 10, 15, and 25 h after wounding to document cell migration across the wound. The results were repeated at least in two batches of experiments.

2.8. Boyden chamber migration assay

Subconfluent TE85, MNNG/HOS, and 143B cells were plated onto a T-25 flask and infected with equivalent titers of either AdS100A6 or AdGFP for 20 h. The cells were harvested and washed with 0.1% BSA serum free media. Pre-equilibrated media containing 5% FCS as a chemoattractant was placed into the bottom chamber of 6-well transwell unit (Corning Costar, Corning, NY). 5×10^4 cells were placed onto each upper chamber of the transwell unit whose polycarbonate 8 µm pore membrane was pre-coated with 0.2 mg/ml of rat tail type I collagen (BD Biosciences, Bedford, MA) overnight and washed in PBS. The cells were allowed to migrate at 37 °C and 5% CO₂ for 4.5 h. The unattached cells were rinsed off with PBS and the membrane containing attached cells were fixed in 10% formalin and washed with PBS. The cells were stained with hematoxylin and rinsed with water. Cells on the unmigrated side were gently wiped off with a wet cotton tip applicator and the membrane was rinsed with water. The membranes containing the migrated cells were

dried, and mounted onto slides with Permount. Six random high power fields (hpf) per membrane were counted for the number of migrate cells. The experiments were repeated with 0.5% FCS as the chemoattractant.

2.9. Collagen gel colony formation assay

Subconfluent TE85, MNNG/HOS, and 143B cells were infected with either AdS100A6 or AdGFP at a comparable titer. At 20 h after infection, the cells were harvested and washed with serum free media. The final concentration of the collagen gel was 1.69 mg/ml of rat tail type I collagen (BD Biosciences), 0.8× DMEM with 5% FCS, and 0.75% NaHCO₃. The bottom layer of the gel was poured and allowed to solidify in a 12-well plate. The top layer containing 8×10³ cells in suspension per well was poured and allowed to solidify. The 1× DMEM containing 5% FCS overlaid the collagen gel to prevent desiccation and the plates were wrapped with plastic wrap. Colonies were allowed to form over 9 days in a 37 °C CO₂ incubator. The assays were done in triplicate.

2.10. Biostatistical analysis

Statistical analyses were performed using STATA version 7 (Stata Corporation, College Station, TX). Kruskal–Wallis or Wilcoxon rank-sum test was used to examine the relationship of S100A6 staining to categorical variables including gender, stage, tumor grade, histologic subtypes, and source of specimen, and *F*-test was used to examine the relationship between S100A6 staining and age. Spearman correlation was used to examine the relationship between S100A6 staining and tumor viability. To clarify the association between metastasis and S100A6, we conducted the analysis in two steps. First, Wilcoxon rank-sum test and Fisher's exact test were used to examine the distribution of S100A6 staining score according to the status of metastasis, ignoring time of metastasis. Second, of patients who were metastasis-free when their specimens were obtained, log-rank test for trend was employed to compare time to metastasis in different groups of S100A6 staining scores, and the risk ratios of developing metastasis were calculated using a Cox proportional hazards

model. The log-rank test for trend was used to compare overall survival time by S100A6 staining score, and a Cox proportional hazards model was used to calculate risk ratios when controlling for the effects of age.

3. Results

3.1. Specificity of the S100A6 antibody

The S100A6 antibody used in this study has been utilized in several earlier studies [36,45–47]. Nevertheless, we performed a Western blot analysis under reducing conditions to verify the specificity of the S100A6 antibody. Subconfluent HEK293 cells were transfected with pHAHA-S100A2, pHAHA-S100A4, pHAHA-S100A6, or pHAHA-S100B. At 24 h after transfection, total cell lysates were collected and tested for S100A6 protein expression using the anti-S100A6 and anti-HA antibodies. As shown in Fig. 1A, the monomeric form of S100A6 was only detected in the pHAHA-S100A6 transfected cells (Fig. 1A, lane 3). Thus, the antibody is specific to S100A6 and does not cross-react to other S100 proteins tested. Interestingly, the endogenous expression level of S100A6 was almost undetectable in HEK293 cells. Fig. 1B shows that all the transfectants express the HA-tagged proteins and serves as loading controls.

3.2. Immunohistochemical analysis of S100A6 expression in human osteosarcoma samples

Fifty specimens corresponding to 50 osteosarcoma patients were evaluated. Immunohistochemical analyses demonstrated that 84% of the specimens (42 of 50) stained positively for S100A6 while 16% (8 of 50) did not exhibit detectable staining (Table 1). Representative samples of specimens with weak 1(+), moderate (2+), and strong (3+) staining for S100A6 are shown in Fig. 1C–E, respectively, with the corresponding goat IgG controls and hematoxylin and eosin stain. The distribution of S100A6 staining patterns was nuclear (57%), cytoplasmic (26%), and both (17%), and did not correlate with patient survival (*P*=0.72) or

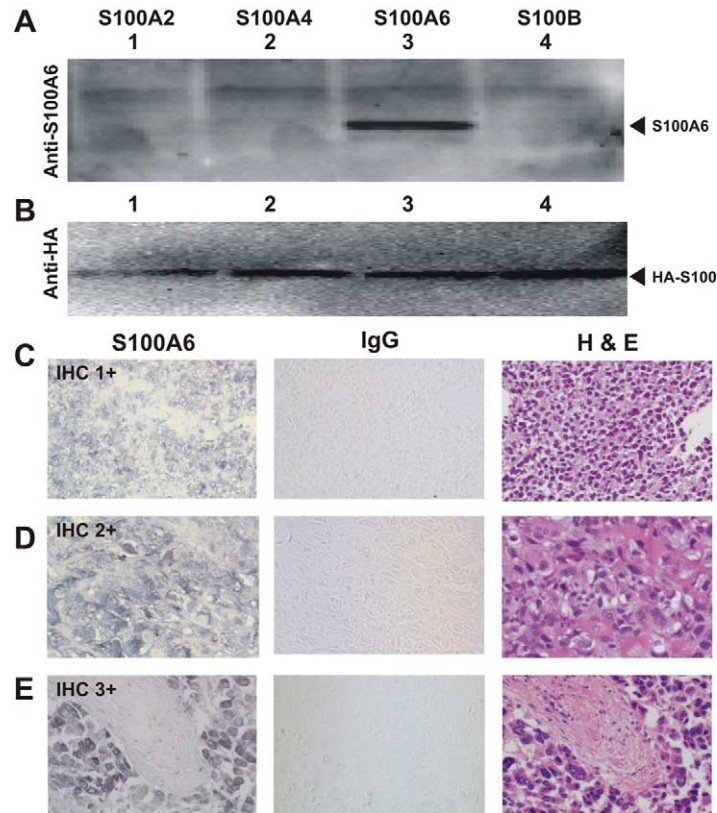


Fig. 1. S100A6 antibody specificity and S100A6 expression in osteosarcoma samples. (A and B) Specificity of the anti-human recombinant S100A6 antibody was verified by Western blot analysis. Subconfluent HEK-293 cells were transfected with vectors expressing HA-tagged S100A2, S100A4, S100A6, and S100B proteins. Cells were lysed and subjected to SDS-PAGE and Western blot analyses under reducing conditions using the anti-S100A6 (A) and anti-HA (B) antibodies. The presence of monomeric S100A6 and HA-tagged S100 proteins (indicated by arrows) was visualized using the SuperSignal West Pico Chemiluminescent Substrate kit (PIERCE). (C–E) Immunohistochemical analysis of S100A6 expression was performed in 50 human osteosarcoma samples. Each selected tumor was accompanied by hematoxylin–eosin (H&E) staining to verify tumor histology. Representative cases with weak (1+), moderate (2+), and strong (3+) staining are shown (C–E, respectively) with the corresponding H&E staining and IgG controls (see text for details).

metastatic disease ($P=0.55$). There were no statistical differences in staining results for gender, age, or grade (Table 1). Statistical analysis demonstrated no significant difference in S100A6 staining among the histologic subtypes (Kruskal–Wallis test, $P=0.19$). The S100A6 staining score was also similar between pre- and post-chemotherapy specimens ($P=0.71$), suggesting that S100A6 expression was not altered by chemotherapy. In addition, from the 26 patients from whom there were data on post-chemotherapy tumor viability, there was no significant correlation between differences in tumor viability and the expression level of S100A6 (Spearman correlation coefficient = -0.11 ,

$P=0.59$). This suggests that the relationship between S100A6 expression and survival or metastasis is not biased by post-chemotherapy tumor viability.

3.3. Survival and the expression level of S100A6

We next examined patient survival with respect to S100A6 staining score in the 50 patients. At the time of the latest follow-up, 29 of 50 patients had died. The median follow-up time for the surviving patients was 84 months. The median survival times for patients with S100A6 staining score of 0, 1, 2, and 3 were 28, 47, 59, and 80 months, respectively

Table 1
Summary of clinicopathological data and S100A6 immunohistochemical analyses on the human osteosarcoma specimens and patients

	Total	S100A6 (–), negative	S100A6 (1+), weak	S100A6 (2+), moderate	S100A6 (3+), strong	<i>P</i> -value*
Total	50	8 (16%)	10 (20%)	14 (28%)	18 (36%)	n/a
<i>Gender</i>						
Male	29	3	6	10	10	0.61
Female	21	5	4	4	8	
Mean age (SD)	32.7 (22.2)	28.1 (17.2)	35.8 (24.5)	34.8 (22.6)	31.5 (23.7)	0.90 ^a
<i>Grade</i>						
High	45	6	10	11	18	0.22
Moderate	1	1	0	0	0	
Low	4	1	0	3	0	
<i>Enneking stage</i>						
IA	1	0	0	1	0	0.4
IB	3	1	0	2	0	
IIA	1	0	0	0	1	
IIB	35	5	5	11	14	
III	10	2	5	0	3	
<i>Chemotherapy</i>						
(–) Chemotherapy	23	2	6	9	6	0.71
(+) Chemotherapy	27	6	4	5	12	
<i>Histologic subtypes</i>						
Chondroblastic	13	2	5	3	3	0.19
Fibroblastic	16	2	1	4	9	
Osteoblastic	15	4	3	4	4	
Telangiectactic	5	0	1	3	1	
Small cell	1	0	0	0	1	

*Unless otherwise specified, *P*-values were calculated using Kruskal–Wallis test or Wilcoxon rank sum test.

^a *P*-value from *F* test.

(Table 2). Since age may be a confounding factor for survival and the range of ages in our group of patients was between 7 and 76 years, we next evaluated patient survival while adjusting for age. In our 50 patients, a 10-year increase in age was associated with a 21% increase in the risk of death ($P=0.017$). This finding is most likely due to confounding co-morbidity since 11 patients were older than 60 years. After adjusting for the potential confounding effects of age, the risk ratio

(RR) for patients with staining scores of 2 or 3 relative to patients with staining scores of 0 or 1 was 0.50 (95% confidence interval, CI, 0.24–1.07; $P=0.074$). Fig. 2A demonstrates the survival curves for our patients with respect to S100A6 expression. When we adjusted for post-chemotherapy tumor viability, the risk ratio was similar (RR=0.58), suggesting that this survival trend was not confounded by post-chemotherapy tumor viability. Therefore, our results suggest a trend towards

Table 2
Correlation between S100A6 immunohistochemical staining and the clinical development of metastases and patient survival ($n=50$)

	S100A6 (–), negative	S100A6 (1+), weak	S100A6 (2+), moderate	S100A6 (3+), strong	<i>P</i> -value*
Metastasis ($n=28$)	6	8	7	7	0.025*
No metastasis ($n=22$)	2	2	7	11	
Median survival (months)	28	47	59	80	0.10 ^a

**P*-value from Wilcoxon rank-sum.

^a Age-adjusted *P*-value examining the trends toward decreased metastasis or increased survival with increased S100A6 staining scores.

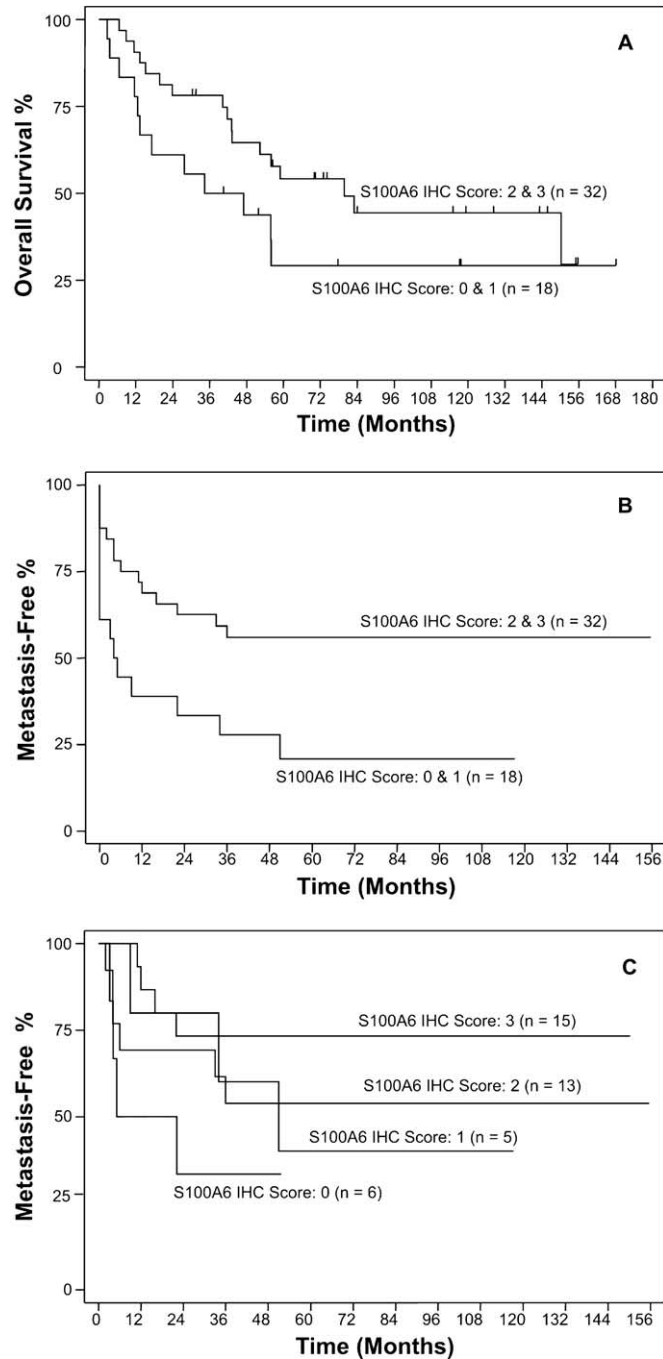


Fig. 2. Biostatistical correlation of S100A6 expression level with survival and clinically evident metastasis (median follow-up: 84 months). (A) Relationship between overall survival and level of S100A6 expression ($n=50$). Although there is a trend towards increased survival with increased S100A6 score, this finding is only borderline statistically significant (age-adjusted $P=0.074$). (B) Relationship of clinically detectable metastasis and S100A6 expression ($n=50$). There is a statistically significant trend towards increased metastasis with decreased S100A6 expression ($P=0.036$). (C) To determine the risk of developing clinically evident metastases, we evaluated the relationship between S100A6 expression and the development of metastasis in patients who were metastasis-free at diagnosis ($n=39$). There is a statistically significant trend towards increased risk of metastasis with decreased S100A6 expression ($P=0.043$).

increased survival with increased S100A6 expression.

3.4. Osteosarcoma metastasis and the expression level of S100A6

We next analyzed the possible correlation between S100A6 staining and metastasis status of our osteosarcoma patients. As shown in Table 2, a total of 28 patients had metastases when the specimens were taken or developed metastases during follow-up. The remaining 22 patients had not developed metastases after at least 32 months of follow-up. As the staining score for S100A6 increased, the proportion of patients with metastases decreased: 6/8, 8/10, 7/14, and 7/18 for staining scores of 0, 1, 2, and 3, respectively ($P=0.025$). When the staining scores 0 and 1 were combined to be defined as low S100A6 expressers and staining scores 2 and 3 were combined to be defined as high S100A6 expressers, again there is a significant trend towards decreased metastasis with increased S100A6 expression ($P=0.036$) (Fig. 2B). Next, we examined the risk of developing metastases in patients who did not have clinically detectable metastases at diagnosis. In this group of 39 patients, 17 patients developed clinical metastases during follow-up. As the staining score for S100A6 increased, the incidence rate of these patients with metastases decreased: 38, 12, 7, and 5% per year for staining scores 0, 1, 2, and 3, respectively. This trend was statistically significant ($P=0.043$) with a risk ratio of 0.65 (95% CI 0.42–1.00) for each one-unit increment in the S100A6 staining score (Fig. 2C). Therefore, increased S100A6 expression appears to predict a decreased risk of metastasis in patients who are metastasis-free at diagnosis. In all of our metastasis analyses, the risk ratio was nearly the same after controlling for post-chemotherapy tumor viability (RR=0.71), age (RR=0.65), or pre-chemotherapy versus post-chemotherapy specimen (RR=0.63). Therefore, the relationship between metastasis and S100A6 expression did not appear to be confounded by these factors.

3.5. S100A6-mediated inhibition of cell migration of osteosarcoma cells

Based on our findings on the relationship between S100A6 expression and osteosarcoma

metastasis, we next proceeded to investigate the functional role of S100A6 in three osteosarcoma cell lines (MNNG/HOS, TE85, and 143B) to elucidate a mechanism by which S100A6 expression is protective against metastatic disease. Adenovirus containing the S100A6 tagged with the green fluorescence protein (GFP) was generated using our previously described AdEasy system [42]. Control GFP adenovirus was also generated. Although the three osteosarcoma lines have some detectable endogenous expression of S100A6 (data not shown), we wanted to test the effects of S100A6 overexpression on cell motility on a wound healing assay. Specifically, subconfluent TE85, MNNG/HOS, and 143B osteosarcoma cells were plated onto a 12-well tissue culture plate and the cells were infected with equal titers of either the AdS100A6 or AdGFP control adenovirus for 20 h. Following the infection, a scratch wound was created across the monolayer and the cells washed with media to remove the remaining viruses and any nonadherent cells. Bright field and fluorescence images of the same fields were taken at 0, 5, 15, and 25 h to monitor the migration in closing the wound (Fig. 3A). Bright field images at time points 0 and 25 h are shown as a reference. A mark on the plate as indicated by the asterisk on the bright field images (Fig. 3A) was created with an 18-gauge needle to ensure that the same field was photographed at each time point. Based on the fluorescence and bright field images, nearly all the cells were expressing our gene of interest. As shown in Fig. 3A, the MNNG/HOS cells overexpressing S100A6 demonstrated less migration compared to the GFP controls. However, the cells infected with the GFP controls were able to nearly re-approximate the wound by 25 h. As expected, the expression of the S100A6 transgene increased over time. The assay was repeated in lower serum conditions (0.5% FCS and 0.1% FCS) as well as in the TE85 and 143B cell lines with similar results (data not shown).

To further test the role of S100A6 on cell motility, we next examined the effects of S100A6 overexpression in a Boyden Chamber migration assay. Briefly, 143B osteosarcoma cells were infected with equal titers of either the AdS100A6 or AdGFP control viruses for 20 h. The cells were harvested, counted,

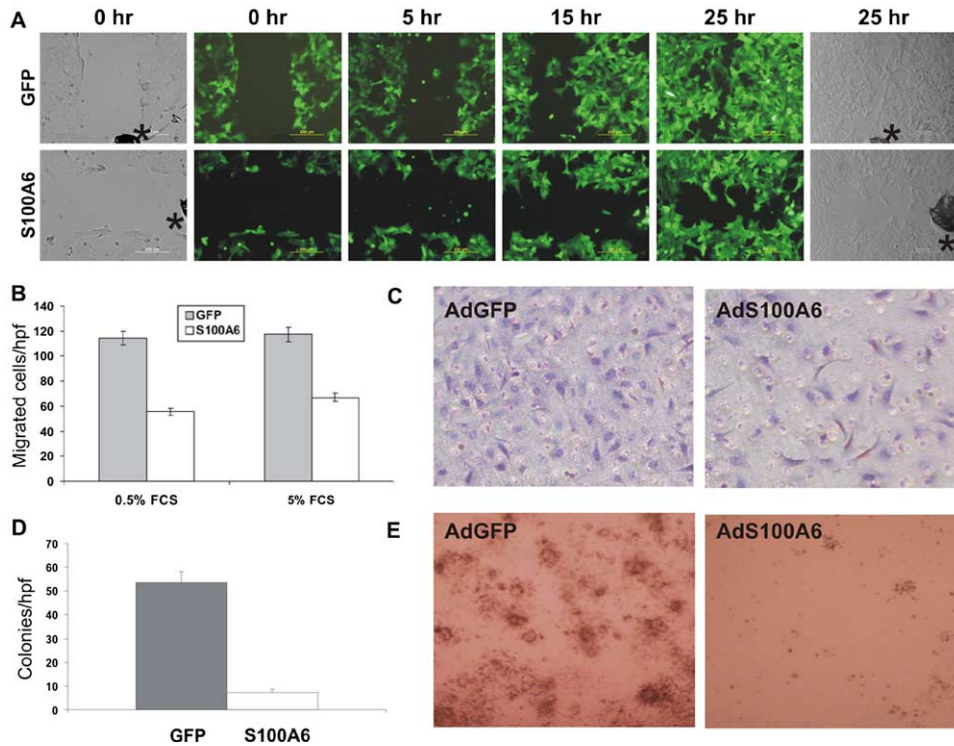


Fig. 3. (A) Wound healing assay on osteosarcoma cells overexpressing S100A6. MNNG/HOS cells were infected with either AdS100A6 or control AdGFP for 20 h in media with 1% FCS. A scratch wound was created across the subconfluent monolayer of cells. Bright field and fluorescence images of the exact field as referenced by a mark made on the plate (asterisk) were taken at 0, 5, 15, and 25 h to observe the migration of the cells across the wound. The experiments were repeated using 0.1 and 0.5% FCS and in TE85 and 143B cells with similar results. (B and C) Boyden Chamber migration assay. Subconfluent 143B cells were infected with AdS100A6 or control AdGFP adenovirus for 20 h and gene expression verified by fluorescence microscopy. A suspension of 5×10^4 infected cells in 0.1% BSA serum free media was placed onto each upper chamber of the transwell unit whose membrane was previously coated with 0.2 mg/ml of rat tail type I collagen. The indicated concentration of FCS was used as a chemoattractant. The cells were allowed to migrate for 4.5 h and the cells were fixed and stained with hematoxylin. The unmigrated cells were removed and the membrane mounted. (B) Number of migrated cells per hpf for S100A6 and GFP expressing cells with the respective chemoattractant concentrations. (C) Representative fields of S100A6 or GFP expressing cells that have migrated across the membrane using 5% FCS as a chemoattractant. (D and E) Collagen gel colony formation assay. A suspension of 8×10^3 infected cells was placed in each well containing a final concentration of 1.69 mg/ml of type I collagen and $0.8 \times$ DME with 5% FCS. Colonies were allowed to form over 9 days. (D) Number of colonies per high field for GFP and S100A6 expressing cells. (E) Representative photographs of colonies formed by S100A6 and GFP expressing cells. The experiments were performed in triplicate.

and plated onto a transwell unit containing a collagen I coated membrane with 8 μ m pores. Fetal calf serum was used as a chemoattractant in the bottom chamber. There was a nearly 2-fold decrease in cell migration with S100A6 overexpression compared to the GFP controls (Fig. 3B). Representative high power fields of the cell that have migrated across the membrane are shown in Fig. 3C. The GFP control has more migrated cells than the S100A6 overexpressing cells (Fig. 3C). The experiments were repeated with a lower serum condition (0.5% FCS) and demonstrated similar

results. The Boyden Chamber migration assays were also performed on the MNNG/HOS and TE85 osteosarcoma cell lines but did not demonstrate a difference that was statistically significant (data not shown). Based on our findings on the wound healing assays on all three cell lines, the inability to detect a significant difference in the MNNG/HOS and TE85 lines may be a reflection of the stringency of the Boyden Chamber migration assay. This is consistent with the fact that 143B is the most aggressive osteosarcoma line among the three lines [48,49].

Nevertheless, these results from the migration assay on the 143B cell line are consistent with the wound healing assay.

3.6. S100A6-mediated inhibition of anchorage independent growth of human osteosarcoma cells

Since our results from the wound healing and Boyden Chamber migration assay suggest that S100A6 may have role on cell adhesion and cell motility, we wanted to examine the role of S100A6 on anchorage independent growth which is a culmination of cell–cell adhesion and tumorigenicity. Osteosarcoma cells overexpressing S100A6 were tested for their ability to form colonies on a type I collagen gel. Briefly, 143B osteosarcoma cells were infected with equal titers of either the AdS100A6 or AdGFP control virus for 20 h. The cells were harvested, counted, and resuspended into a type I collagen gel. Colonies readily formed in 9 days and photographs were taken for colony counting. The assay was performed in triplicate. As shown in Fig. 3D, there appears to be a nearly 8-fold difference between the AdGFP and AdS100A6 infected cells. Fig. 3E is representative fields containing 143B cells infected with AdGFP and AdS100A6, respectively. Interestingly, the MNNG/HOS and the TE85 osteosarcoma cell lines did not readily form colonies when examined (data not shown), which is consistent with the results from the Boyden Chamber migration assay. In addition, a tetrazolium MTS cell proliferation assay was performed and did not show any difference in cell proliferation with respect to S100A6 expression in all three osteosarcoma lines examined in this investigation (data not shown). Nevertheless, S100A6 overexpression appears to inhibit anchorage independent growth in a collagen gel in the 143B osteosarcoma cell line.

4. Discussion

In this study, we have demonstrated that 84% of the examined osteosarcoma specimens expressed S100A6. Furthermore, increased expression of S100A6 correlated with a significantly lower rate of metastasis in our investigation. Survival analysis suggests a trend towards increased survival with

increased expression of S100A6. Although the survival trend is consistent with our findings on the metastasis analysis, our survival analysis was not statistically significant (adjusted $P=0.074$). To further characterize the functional role of S100A6 in human osteosarcoma, we overexpressed S100A6 in three osteosarcoma lines (TE85, MNNG/HOS and 143B) and demonstrated that S100A6 overexpression correlated with decreased cell motility and anchorage independent growth. However, S100A6 overexpression did not alter cell proliferation as determined by MTS assays.

Our immunohistochemical findings are consistent with the work by Muramatsu et al., who in a cross-sectional analysis of S100A6 expression in a variety of tumors found that the three osteosarcoma specimens analyzed demonstrated moderate to strong staining for S100A6 [45]. To our knowledge, our study is the first report of S100A6 expression in a fairly large series of osteosarcoma specimens. Our findings are also consistent with the findings by Rehman et al. who examined S100A6 expression in benign, premalignant, malignant, and metastatic prostate tissues [50]. The authors noticed that S100A6 was highly expressed in benign prostatic epithelium but its expression was lost in matched adenocarcinomas and metastatic lesions. In our series of patients, decreased S100A6 expression correlated with increase metastases. This is also consistent with our in vitro assays in which increase S100A6 expression was associated with decreased motility and decreased anchorage independent growth in a type I collagen gel.

While little is known about the exact functional role of S100A6, it has been shown to interact with the actin cytoskeleton via tropomyosin [25,51]. The actin microfilament system attaches to the adherens junctions and is involved in cell contractility and adhesion dependent signaling with the extracellular matrix [52]. It is conceivable that through its interactions with the actin microfilament system, S100A6 can modulate cell adhesion, cell motility, and/or anchorage independent growth. Interestingly, tropomyosin has been shown to suppress transformed phenotypes, such as anchorage independent growth, in both ras and src transformed cells [53–55]. Our findings on the role of S100A6 on cell motility and anchorage independent growth in osteosarcoma cells are consistent with

these reports. Although the lineage of osteosarcoma cells is uncertain, S100A6 is expressed in mature osteoblasts and is upregulated upon exogenous stimulation for osteoblastic differentiation [56,57]. Perhaps the loss of S100A6 expression may be involved in the progression of human osteosarcoma and is associated with an aggressive phenotype.

Interestingly, our results differ from those by Komatsu et al. and Maelandsmo et al., who have found that increased expression of S100A6 is correlated with metastasis in colon cancer and melanoma, respectively [27,46,58]. However, in a subsequent study with patient-matched samples, Komatsu et al. found S100A6 expression in the primary tumor, but there was no statistical difference in S100A6 expression between the primary tumor and the liver metastases [47]. In fact, the expression of S100A6 was similar or even reduced in the majority of the liver metastases compared to the primary tumor when analyzed by immunohistochemistry, which would be consistent with our results [47]. Nevertheless, our findings suggest that S100A6 expression is common in human osteosarcoma.

One of the limitations of our study is that we included both pre- and post-chemotherapy specimens as a result of the random selection of our specimens. This would be especially relevant if S100A6 expression in osteosarcoma were affected by chemotherapy. However, when we compared the presence or absence of chemotherapy with S100A6 expression, we did not see a statistical difference, suggesting that S100A6 expression was not altered by chemotherapy. Furthermore, analysis of the available tumor viability data suggests that neither the administration of chemotherapy nor the response to chemotherapy affected the relationship between S100A6 expression and metastasis or survival. In addition, we were not able to detect a correlation between tumor grade/stage and S100A6 expression as would be expected. This is most likely attributed to the fact that the vast majority of our specimens were high grade with advanced stages, and therefore we would require considerably more samples to be able to detect a difference.

Although we see a trend towards increased survival with increased S100A6 expression, this was not statistically significant (age-adjusted $P=0.074$). The inability to detect a significant difference may be due

to our sample size of 50 and/or may reflect our improving ability to treat patient with metastatic disease surgically and chemotherapeutically and thereby improving patient survival. Interestingly, the survival rate in our group of patients is lower than expected. This is likely due to the fact that we included samples from older patients as well as samples from patients with advanced stages. Bielack et al. report a 10-year survival of 41.6% in patients older than 40 years [59]. In addition, 28/50 of our patients had or developed metastatic disease. Although the samples were randomly, this atypical distribution may contribute to our lower survival rate.

Taken together, our results demonstrate that S100A6 is highly expressed in human osteosarcoma but increased S100A6 expression correlates with a decreased rate of metastasis, cell motility, and anchorage independent growth. These results suggest that S100A6 can be explored as a potential marker for osteosarcoma as it pertains to metastatic disease since the loss of its expression may be an unfavorable event. As we understand more about the role of S100A6 in human osteosarcoma, its expression may help to stratify a patient's risk of future metastasis. This knowledge could potentially alter the treatment algorithm in these patients such as the need for post-operative chemotherapy and thereby reduce the wound and systemic complications associated with chemotherapy. In this regard, S100A6 expression could be considered a favorable outcome marker for osteosarcoma patients.

Acknowledgements

We would like to thank the staff at The University of Chicago Cancer Registry for their valuable assistance. This work was supported in part by research grants from The Brinson Foundation, the Orthopedic Research and Education Foundation, and the National Institutes of Health. Hue H. Luu was a recipient of the OREF Resident Research Award.

References

- [1] M.D. Murphey, M.R. Robbin, G.A. McRae, D.J. Flemming, H.T. Temple, M.J. Kransdorf, The many faces of osteosarcoma, *Radiographics* 17 (1997) 1205–1231.

- [2] J.S. Whelan, Osteosarcoma, *Eur. J. Cancer* 33 (1997) 1611–1618 discussion; 1618–1619.
- [3] S.M. Bentzen, H.S. Poulsen, S. Kaae, O.M. Jensen, H. Johansen, H.T. Mouridsen, et al., Prognostic factors in osteosarcomas. A regression analysis, *Cancer* 62 (1988) 194–202.
- [4] A.M. Davis, R.S. Bell, P.J. Goodwin, Prognostic factors in osteosarcoma: a critical review, *J. Clin. Oncol.* 12 (1994) 423–431.
- [5] M.P. Link, A.M. Goorin, A.W. Miser, A.A. Green, C.B. Pratt, J.B. Belasco, et al., The effect of adjuvant chemotherapy on relapse-free survival in patients with osteosarcoma of the extremity, *N. Engl. J. Med.* 314 (1986) 1600–1606.
- [6] W.G. Ward, K. Mikaelian, F. Dorey, J.M. Mirra, A. Sassoon, E.C. Holmes, et al., Pulmonary metastases of stage IIB extremity osteosarcoma and subsequent pulmonary metastases, *J. Clin. Oncol.* 12 (1994) 1849–1858.
- [7] S.C. Kaste, C.B. Pratt, A.M. Cain, D.J. Jones-Wallace, B.N. Rao, Metastases detected at the time of diagnosis of primary pediatric extremity osteosarcoma at diagnosis: imaging features, *Cancer* 86 (1999) 1602–1608.
- [8] T. Yonemoto, S. Tatezaki, T. Ishii, T. Satoh, H. Kimura, N. Iwai, Prognosis of osteosarcoma with pulmonary metastases at initial presentation is not dismal, *Clin. Orthop.* 1998; 194–199.
- [9] W.S. Ferguson, A.M. Goorin, Current treatment of osteosarcoma, *Cancer Invest.* 19 (2001) 292–315.
- [10] G.D. Letson, C.A. Muro-Cacho, Genetic and molecular abnormalities in tumors of the bone and soft tissues, *Cancer Control* 8 (2001) 239–251.
- [11] B.D. Ragland, W.C. Bell, R.R. Lopez, G.P. Siegal, Cytogenetics and molecular biology of osteosarcoma, *Lab. Invest.* 82 (2002) 365–373.
- [12] B. Fuchs, D.J. Pritchard, Etiology of osteosarcoma, *Clin. Orthop.* 2002; 40–52.
- [13] J.A. Bridge, M. Nelson, E. McComb, M.H. McGuire, H. Rosenthal, G. Vergara, et al., Cytogenetic findings in 73 osteosarcoma specimens and a review of the literature, *Cancer Genet. Cytogenet.* 95 (1997) 74–87.
- [14] A. Forus, J.M. Berner, L.A. Meza-Zepeda, G. Saeter, D. Mischke, O. Fodstad, et al., Molecular characterization of a novel amplicon at 1q21-q22 frequently observed in human sarcomas, *Br. J. Cancer* 78 (1998) 495–503.
- [15] T. Ozaki, K.L. Schaefer, D. Wai, H. Buerger, S. Flege, N. Lindner, et al., Genetic imbalances revealed by comparative genomic hybridization in osteosarcomas, *Int. J. Cancer* 102 (2002) 355–365.
- [16] B.W. Schafer, C.W. Heizmann, The S100 family of EF-hand calcium-binding proteins: functions and pathology, *Trends Biochem. Sci.* 21 (1996) 134–140.
- [17] A. Lewit-Bentley, S. Rety, EF-hand calcium-binding proteins, *Curr. Opin. Struct. Biol.* 10 (2000) 637–643.
- [18] R. Donato, S100: a multigenic family of calcium-modulated proteins of the EF-hand type with intracellular and extracellular functional roles, *Int. J. Biochem. Cell Biol.* 33 (2001) 637–668.
- [19] C.W. Heizmann, G. Fritz, B.W. Schafer, S100 proteins: structure, functions and pathology, *Front. Biosci.* 7 (2002) d1356–d1368.
- [20] I. Marenholz, C.W. Heizmann, G. Fritz, S100 proteins in mouse and man: from evolution to function and pathology (including an update of the nomenclature), *Biochem. Biophys. Res. Commun.* 322 (2004) 1111–1122.
- [21] B.W. Moore, A soluble protein characteristic of the nervous system, *Biochem. Biophys. Res. Commun.* 19 (1965) 739–744.
- [22] R.S. Mani, W.D. McCubbin, C.M. Kay, Calcium-dependent regulation of caldesmon by an 11-kDa smooth muscle calcium-binding protein, caltropin, *Biochemistry* 31 (1992) 11896–11901.
- [23] G. Sorci, A.L. Agneletti, R. Bianchi, R. Donato, Association of S100B with intermediate filaments and microtubules in glial cells, *Biochim. Biophys. Acta* 1448 (1998) 277–289.
- [24] M. Garbuglia, M. Verzini, G. Sorci, R. Bianchi, I. Giambanco, A.L. Agneletti, et al., The calcium-modulated proteins, S100A1 and S100B, as potential regulators of the dynamics of type III intermediate filaments, *Braz. J. Med. Biol. Res.* 32 (1999) 1177–1185.
- [25] N.L. Golitsina, J. Kordowska, C.L. Wang, S.S. Lehrer, Ca²⁺-dependent binding of calyculin to muscle tropomyosin, *Biochem. Biophys. Res. Commun.* 220 (1996) 360–365.
- [26] M. Garbuglia, M. Verzini, R. Donato, Annexin VI binds S100A1 and S100B and blocks the ability of S100A1 and S100B to inhibit desmin and GFAP assemblies into intermediate filaments, *Cell Calcium* 24 (1998) 177–191.
- [27] G.M. Maelandsmo, V.A. Florenes, T. Mellingsaeter, E. Hovig, R.S. Kerbel, O. Fodstad, Differential expression patterns of S100A2, S100A4 and S100A6 during progression of human malignant melanoma, *Int. J. Cancer* 74 (1997) 464–469.
- [28] L. Lauriola, F. Michetti, N. Maggiano, J. Galli, G. Cadoni, B.W. Schafer, et al., Prognostic significance of the Ca²⁺ binding protein S100A2 in laryngeal squamous-cell carcinoma, *Int. J. Cancer* 89 (2000) 345–349.
- [29] D. Liu, P.S. Rudland, D.R. Sibson, A. Platt-Higgins, R. Barraclough, Expression of calcium-binding protein S100A2 in breast lesions, *Br. J. Cancer* 83 (2000) 1473–1479.
- [30] W. El-Rifai, C.A. Moskaluk, M.K. Abdrabbo, J. Harper, C. Yoshida, G.J. Riggins, et al., Gastric cancers overexpress S100A calcium-binding proteins, *Cancer Res.* 62 (2002) 6823–6826.
- [31] K. Kimura, Y. Endo, Y. Yonemura, C.W. Heizmann, B.W. Schafer, Y. Watanabe, et al., Clinical significance of S100A4 and E-cadherin-related adhesion molecules in non-small cell lung cancer, *Int. J. Oncol.* 16 (2000) 1125–1131.
- [32] K.B. Pedersen, J.M. Nesland, O. Fodstad, G.M. Maelandsmo, Expression of S100A4, E-cadherin, alpha- and beta-catenin in breast cancer biopsies, *Br. J. Cancer* 87 (2002) 1281–1286.
- [33] K. Takenaga, Suppression of metastasis-associated S100A4 gene expression by gamma- interferon in human colon adenocarcinoma cells, *Br. J. Cancer* 80 (1999) 127–132.

- [34] I. Ninomiya, T. Ohta, S. Fushida, Y. Endo, T. Hashimoto, M. Yagi, et al., Increased expression of S100A4 and its prognostic significance in esophageal squamous cell carcinoma, *Int. J. Oncol.* 18 (2001) 715–720.
- [35] O. Ben-Izhak, P. Stark, R. Levy, R. Bergman, C. Lichtig, Epithelial markers in malignant melanoma. A study of primary lesions and their metastases, *Am. J. Dermatopathol.* 16 (1994) 241–246.
- [36] E.C. Ilg, B.W. Schafer, C.W. Heizmann, Expression pattern of S100 calcium-binding proteins in human tumors, *Int. J. Cancer* 68 (1996) 325–332.
- [37] A.W. Barrett, C. Scully, S100 protein in oral biology and pathology, *J. Oral. Pathol. Med.* 23 (1994) 433–440.
- [38] B. Mathisen, R.I. Lindstad, J. Hansen, S.A. El-Gewely, G.M. Maelandsmo, E. Hovig, et al., S100A4 regulates membrane induced activation of matrix metalloproteinase-2 in osteosarcoma cells, *Clin. Exp. Metastasis* 20 (2003) 701–711.
- [39] D.R. Fullen, J.A. Reed, B. Finnerty, N.S. McNutt, S100A6 expression in fibrohistiocytic lesions, *J. Cutan. Pathol.* 28 (2001) 229–234.
- [40] R.C. Haydon, A. Deyrup, A. Ishikawa, R. Heck, W. Jiang, L. Zhou, et al., Cytoplasmic and/or nuclear accumulation of the beta-catenin protein is a frequent event in human osteosarcoma, *Int. J. Cancer* 102 (2002) 338–342.
- [41] A.T. Deyrup, R.C. Haydon, D. Huo, A. Ishikawa, T.D. Peabody, T.C. He, et al., Myoid differentiation and prognosis in adult pleomorphic sarcomas of the extremity: an analysis of 92 cases, *Cancer* 98 (2003) 805–813.
- [42] T.C. He, S. Zhou, L.T. da Costa, J. Yu, K.W. Kinzler, B. Vogelstein, A simplified system for generating recombinant adenoviruses, *Proc. Natl Acad. Sci. USA* 95 (1998) 2509–2514.
- [43] Y. Peng, Q. Kang, Q. Luo, W. Jiang, W. Si, B.A. Liu, et al., Inhibitor of DNA binding/differentiation helix-loop-helix proteins mediate bone morphogenetic protein-induced osteoblast differentiation of mesenchymal stem cells, *J. Biol. Chem.* 279 (2004) 32941–32949.
- [44] Q. Luo, Q. Kang, W. Si, W. Jiang, J.K. Park, Y. Peng, et al., Connective tissue growth factor (CTGF) is regulated by Wnt and bone morphogenetic proteins signaling in osteoblast differentiation of mesenchymal stem cells, *J. Biol. Chem.* 279 (2004) 55958–55968.
- [45] Y. Muramatsu, A. Kamegai, T. Shiba, P. Shrestha, Y. Takai, M. Mori, et al., Histochemical characteristics of calcium binding S100 proteins and bone morphogenetic proteins in chondro-osseous tumors, *Oncol. Rep.* 1997; 49–53.
- [46] K. Komatsu, Y. Kobune-Fujiwara, A. Andoh, S. Ishiguro, H. Hunai, N. Suzuki, et al., Increased expression of S100A6 at the invading fronts of the primary lesion and liver metastasis in patients with colorectal adenocarcinoma, *Br. J. Cancer* 83 (2000) 769–774.
- [47] K. Komatsu, K. Murata, M. Kameyama, M. Ayaki, M. Mukai, S. Ishiguro, et al., Expression of S100A6 and S100A4 in matched samples of human colorectal mucosa, primary colorectal adenocarcinomas and liver metastases, *Oncology* 63 (2002) 192–200.
- [48] J.S. Rhim, D.L. Putman, P. Arnstein, R.J. Huebner, R.M. McAllister, Characterization of human cells transformed in vitro by *N*-methyl-*N'*-nitro-*N*-nitrosoguanidine, *Int. J. Cancer* 19 (1977) 505–510.
- [49] P.J. Hensler, L.A. Annab, J.C. Barrett, O.M. Pereira-Smith, A gene involved in control of human cellular senescence on human chromosome 1q, *Mol. Cell. Biol.* 14 (1994) 2291–2297.
- [50] I. Rehman, S.S. Cross, A.R. Azzouzi, J.W. Catto, J.C. Deloulme, S. Larre, et al., S100A6 (Calcyclin) is a prostate basal cell marker absent in prostate cancer and its precursors, *Br. J. Cancer* 91 (2004) 739–744.
- [51] E.C. Breen, K. Tang, Calcyclin (S100A6) regulates pulmonary fibroblast proliferation, morphology, and cytoskeletal organization in vitro, *J. Cell. Biochem.* 88 (2003) 848–854.
- [52] G. Pawlak, D.M. Helfman, Cytoskeletal changes in cell transformation and tumorigenesis, *Curr. Opin. Genet. Dev.* 11 (2001) 41–47.
- [53] G.L. Prasad, R.A. Fuldner, H.L. Cooper, Expression of transduced tropomyosin 1 cDNA suppresses neoplastic growth of cells transformed by the ras oncogene, *Proc. Natl Acad. Sci. USA* 90 (1993) 7039–7043.
- [54] G.L. Prasad, L. Masuelli, M.H. Raj, N. Harindranath, Suppression of src-induced transformed phenotype by expression of tropomyosin-1, *Oncogene* 18 (1999) 2027–2031.
- [55] R.A. Janssen, J.W. Mier, Tropomyosin-2 cDNA lacking the 3' untranslated region riboregulator induces growth inhibition of v-Ki-ras-transformed fibroblasts, *Mol. Biol. Cell* 8 (1997) 897–908.
- [56] Q. Tu, M. Pi, L.D. Quarles, Calcyclin mediates serum response element (SRE) activation by an osteoblastic extracellular cation-sensing mechanism, *J. Bone Miner. Res.* 18 (2003) 1825–1833.
- [57] R. Hwang, E.J. Lee, M.H. Kim, S.Z. Li, Y.J. Jin, Y. Rhee, et al., Calcyclin, a Ca²⁺ ion-binding protein, contributes to the anabolic effects of simvastatin on bone, *J. Biol. Chem.* 279 (2004) 21239–21247.
- [58] K. Komatsu, A. Andoh, S. Ishiguro, N. Suzuki, H. Hunai, Y. Kobune-Fujiwara, et al., Increased expression of S100A6 (Calcyclin), a calcium-binding protein of the S100 family, in human colorectal adenocarcinomas, *Clin. Cancer Res.* 6 (2000) 172–177.
- [59] S.S. Bielack, B. Kempf-Bielack, G. Delling, G.U. Exner, S. Flege, K. Helmke, et al., Prognostic factors in high-grade osteosarcoma of the extremities or trunk: an analysis of 1,702 patients treated on neoadjuvant cooperative osteosarcoma study group protocols, *J. Clin. Oncol.* 20 (2002) 776–790.